Title

The neural representation of sensorimotor transformations in a human perceptual decision making network

Authors

Erickson, DT
Kayser, AS

Publication Date

2013-10-01

DOI

10.1016/j.neuroimage.2013.04.085

NeuroImage 79 (2013) 340–350

Contents lists available at SciVerse ScienceDirect

NeuroImage

journal homepage: www.elsevier.com/locate/ynimg

The neural representation of sensorimotor transformations in a human perceptual decision making network

Drew T. Erickson [a,b,*], Andrew S. Kayser [a,b,c]

[a] Department of Neurology, University of California, San Francisco, USA
[b] Ernest Gallo Clinic & Research Center, Emeryville, CA 94608, USA
[c] Department of Neurology, VA Northern California Health Care System, Martinez, CA 94553, USA

ARTICLE INFO

Article history:
Accepted 16 April 2013
Available online 28 April 2013

Keywords:
Motion coherence
Perceptual decision making
Sensorimotor transformations
Intraparietal sulcus
fMRI

ABSTRACT

Humans can quickly engage a neural network to transform complex visual stimuli into a motor response. Activity from a key region within this network, the intraparietal sulcus (IPS), has been associated with evidence accumulation and motor planning, thus implicating it in sensorimotor transformations. If such transformations occur within a brain region, a key and untested prediction is that neural activity reflecting both the parametric amount of evidence available and the timing of motor planning can be independently manipulated. To investigate these ideas, we constructed a dot motion discrimination task in which information about response modality (what to use) and response mapping (how to use it) was provided independently either before or after presentation of a dot motion coherence stimulus whose strength varied across trials. Consistent with our hypothesis, activity within IPS covaried with dot motion coherence during the stimulus phase, and as information necessary for the response was delayed, the peak of IPS activity shifted to the response phase. In contrast, areas such as the motion-sensitive region MT+ and the supplementary motor area demonstrated activity limited to the stimulus and response phases of the task, respectively. These results show that activity in IPS correlates with temporally dissociable representations consistent with both evidence accumulation and motor planning, and suggest that IPS is a core component for sensorimotor transformations within the perceptual decision-making network.

Introduction

The ability to link sensation with action is integral to even the most fundamental of decisions. In humans, a number of studies have identified a frontoparietal network involved in processes during perceptual decisions, including sensory processing, attentional control, evidence accumulation, and motor planning (Heekeren et al., 2008; Kayser et al., 2010a,b; Liu and Pleskac, 2011; Ploran et al., 2007, 2011; Rowe et al., 2010; Ho et al., 2009; Tosoni et al., 2008). Previously we demonstrated that for subjects performing a dot motion discrimination task, this network displays a blood oxygen level-dependent (BOLD) response that varies inversely with motion coherence (Kayser et al., 2010a). Consistent with previous and subsequent findings (e.g., Hebart et al., 2012; Ho et al., 2009; Kayser et al., 2010b), this negative parametric effect matched predictions of a proportional-rate diffusion model for evidence accumulation to a threshold (Palmer et al., 2005; Ratcliff and McKoon, 2008), and linked human brain activity with a computational model of the transformation from stimulus to response.

Although this parametric effect is necessary, it is not sufficient to define regions that support such sensorimotor transformations. Human studies, for example, show that areas such as the motion-sensitive region MT+, supplementary motor area (SMA), and intraparietal sulcus (IPS) all display this parametric effect. Importantly, results from macaque studies show that activity in lateral intraparietal area (LIP), the macaque homologue of IPS (Grefkes and Fink, 2005), accords with predictions of the diffusion model and covaries with behavior (Roitman and Shadlen, 2002), consistent with previous macaque work demonstrating a link between LIP activity and response selection (reviewed in Andersen et al., 1997). In contrast, recordings in the macaque homologues of MT+ and SMA implicate them in either sensory (Gold and Shadlen, 2007) or motor (Mita et al., 2009) tasks, respectively. These results suggest that IPS may participate in sensorimotor transformations in humans.

In keeping with the demonstrated findings in LIP, an approach to identify human brain regions directly involved in sensorimotor transformations must show that their activity links both sensory and motor processes. In addition to including both sensory- and motor-related signals, the BOLD correlates of sensorimotor processing in these regions should be temporally dissociable. Specifically, a region important for sensorimotor transformations should show both (1) a maximal parametric variation with the stimulus when evidence accumulation occurs during stimulus presentation, and (2) a dissociable component linked

* Corresponding author at: Dept. of Neurology, U.C. San Francisco, Ernest Gallo Clinic & Research Center, 5858 Horton Street, Suite 200, Emeryville, CA 94608, USA. Fax: +1 510 985 3101.
E-mail address: drew.t.erickson@gmail.com (D.T. Erickson).

1053-8119/$ – see front matter © 2013 Elsevier Inc. All rights reserved.
http://dx.doi.org/10.1016/j.neuroimage.2013.04.085

to motor planning whose timing shifts based on when such planning occurs behaviorally. In contrast, regardless of the timing of motor planning, a region whose activity represents effects of a sensory process such as perceptual salience should demonstrate activity in the presence of the stimulus but minimal activity during the response phase, while an area whose activity represents the implementation of motor plans should be significantly active during the response phase but minimally so during the stimulus phase. Consistent with its role in attention (Kayser et al., 2010b) and action planning, recent work demonstrated that the IPS is active during both sensory and motor phases when responses are delayed (Ho et al., 2009; Liu and Pleskac, 2011; Tosoni et al., 2008). However, definitively identifying regional brain activity consistent with sensorimotor transformations requires that the related cognitive components bridging sensory and motor phases of the task be dissociated. Characterizing such co-localized activity necessitates a task design that can distinguish a parametric stimulus-related activity associated with evidence accumulation from a peak response activity that shifts temporally with motor planning.

To search for regions with activity consistent with sensorimotor transformations, we utilized a modified version of a motion discrimination task that included a parametrically varied motion stimulus and manipulated the timing of information required for planning either a button press or saccadic response to indicate the motion direction of the stimulus. Specifically, cues for modality and mapping required for response were provided independently either before or after stimulus presentation, thus delaying motor planning on trials in which information was withheld. We hypothesized that when response information was withheld, areas involved in sensorimotor transformations would show activity correlated parametrically with motion coherence during the stimulus phase, and distinct activity that shifted to the response phase when motor planning was delayed. However, areas involved primarily in sensory processing or motor implementation would show activity restricted to either the sensory or response phase, irrespective of the timing of response information.

Methods

Subject training and task performance

Seven subjects (ages 18–24, 3 male) participated in the study and gave written informed consent in accordance with the Committee for the Protection of Human Subjects at the University of California, Berkeley. All subjects had normal neuroanatomy as reviewed by a neurologist (A.S.K.), were right-handed, and had normal or corrected-to-normal vision. Prior to any scan sessions, subjects were trained on the task in a 1.5-hour behavioral session to reduce both the number of invalid trials and learning effects in the scanner. In the following days, subjects underwent five 1.5-hour fMRI task sessions, consisting of 12 runs of 24 trials for a total of $5 \times 12 \times 24 = 1440$ trials. We chose to scan a small number of highly trained subjects across multiple days in order to maximize our ability to detect parametric changes in the BOLD signal within all conditions, as in other visual studies (Amano et al., 2009; Lee et al., 2007; Silver et al., 2008) and our own previous studies (Kayser et al., 2010a,b).

Subjects performed a visual dot motion task with a delayed response on a stimulus consisting of multiple moving dots. For all trials, a subset of dots moved coherently upward or downward on a background of randomly moving dots. Coherent motion values used for a given trial were 0%, 2%, 4%, 16%, 32%, or 100%. Coherence values were balanced within sessions such that subjects viewed equal numbers of each motion coherence and upward/downward motion in a randomized and independent fashion.

Three types of tasks were constructed based on information provided to the subject in a prompt prior to onset of the dot motion stimulus. The prompt contained either information on modality and mapping (All), modality only (Modality) or no information (None). The remaining information was provided (while previous information was not) during the delayed response phase. Based on the mapping of upward/downward motion to left/right responses, subjects were required to give either a "left" or "right" response using only the appropriate modality when prompted. For a given run of 24 trials, all trials were of one task type (All, Modality, or None). Each session contained equal numbers of task types and their order was randomized.

A trial began with dimming of the fixation cross and appearance of an information cue for 2 s. The cue consisted of either a modality icon (to indicate hand or eye) or a fixation cross (to convey no information), and either left/right arrows above/below the fixation cross (to indicate how motion direction mapped to a left/right response) or filled circles in the corresponding positions (to convey no information). Thus, the cue displayed the images for modality and mapping (All), modality only (Modality), or no information (None). After 2 s, to prevent subjects from anticipating the onset of the response phase, the images dimmed for an interstimulus interval of 2–5 s, based on randomly generated values from a gamma distribution for which 75% of values were within 2–3.5 s. The dot motion stimulus then appeared for 2 s. Afterward, both stimulus and information images were replaced with a dim fixation cross for an interstimulus interval of 2–5 s. A response prompt that consisted of two circular targets each 10° left and right of central fixation then appeared. Any previously undisplayed modality and mapping information was displayed centrally to enable the subject's response, and any previously provided information was withheld in order to ensure that subjects adhered to the task-appropriate strategy. To respond, subjects used the trial-specified modality and mapping information. This response was either a button press with the 2nd or 3rd finger of the right hand before the end of the response prompt, or a saccade to the left or right target. During button presses, subjects were directed to maintain central fixation. During saccades, subjects held their gaze on the specified target until it disappeared, then returned to central fixation. Lastly, the fixation cross brightened and an interstimulus interval of 4–12 s preceded the next trial.

Eye movement data was collected using a ViewPoint EyeTracker (Close-Focus Camera and Illuminator, http://www.arringtonresearch.com). As in our previous studies (Kayser et al., 2010a,b), subjects were trained through verbal feedback to maintain an eye position within 3° of the fixation cross, and to refrain from blinking throughout the duration of the stimulus. Relatively stringent criteria were used to train subjects to maintain fixation and avoid blinks during the stimulus interval. Blinks were classified as any instances in which the pupil aspect ratio was equal to zero for more than 8.3 ms. Eye movements were defined as any period lasting more than 180 ms in which the eye position was greater than 3° from fixation. Subject performance was well within acceptable ranges (fewer than 2% of trials compromised by blinks or eye movements).

Saccade responses were determined through analysis of the eye movement data. Pupil position data taken from the response phase first required temporal smoothing to remove high frequency noise. These data were then examined for movement along the x-axis to either the left or right target that was subsequently held at the target for the remainder of the phase. Movement towards a target was measured from a baseline position determined by the x-axis positional average 1.5 s prior to the response phase. The saccade response time was calculated as the time a movement from the baseline position stabilized at the target x-axis position (zero velocity). Because of the necessary removal of high frequencies in our data, which reduced noise but also reduced resolution for movement onsets and offsets, our reaction times for eye movements are likely to be greater than standard calculations for reaction times. Movements that did not hold position at the target throughout the remaining time or reach the target during the response phase were considered missed responses.

The task was programmed in MATLAB using components of PsychToolbox (Brainard, 1997; Pelli, 1997). The code for the dot motion

display was heavily adapted from an implementation originally written by McKinley and Shadlen and available on the PsychToolbox website (http://psychtoolbox.org/PTB-2/). Stimulus frames were presented within a central 7.5° aperture at 60 frames/s. Dot density was fixed at 16.7 dots/$^{\circ 2}$/s, and dot velocity was fixed at a single value of 5 °/s to ensure that motion energy was uniform across levels of motion coherence. Coherent motion took place in a predetermined upward or downward direction, while the remaining random dot motion was distributed uniformly from 0 to 360°. Motion coherence was distributed across the full dot set, preventing subjects from making accurate decisions based solely on the behavior of a single dot or set of dots. We previously demonstrated that the mean coherence across all frames for a given trial well-approximates the desired coherence (Kayser et al., 2010a). Blurring effects (in which consecutive placements of a single dot were seen as forming a line) were avoided via the serial presentation of three interleaved subsets, with each frame containing only one of the subsets. To ensure that dots were initially placed evenly across the viewing aperture, we rejected initial dot placements that showed evidence for an unusually skewed starting configuration, as in our previous studies (Kayser et al., 2010a,b). Once set in motion, dots that moved outside the aperture were repositioned on the opposite side of the window to prevent them from collecting in any particular region of the aperture over time.

MRI scanning

MRI scanning was conducted on a Siemens MAGNETOM Trio 3T MR Scanner at the Henry H. Wheeler Jr. Brain Imaging Center at the University of California, Berkeley. Anatomical images consisted of 160 slices acquired using a T1-weighted MP-RAGE protocol (TR = 2300 ms, TE = 2.98 ms, FOV = 256 mm, matrix size = 256 × 256, voxel size = 1 mm^3). Functional images consisted of 24 slices acquired with a gradient echoplanar imaging protocol (TR = 1370 ms, TE = 27 ms, FOV = 225 mm, matrix size = 96 × 96, voxel size = 2.3 × 2.3 × 3.5 mm). A projector (Avotec SV-6011, http://www.avotec.org) was used to display the image on a translucent screen placed within the scanner bore behind the head coil. A mirror was used to allow the subject to see the display. The distance from the subject's eye to the screen was 28 cm. Subjects' responses were recorded via a MRI-safe fiber optic response pad (Inline Model HH-1x4-L, http://www.crsltd.com) and a ViewPoint EyeTracker (Close-Focus Camera and Illuminator, http://www.arringtonresearch.com).

fMRI preprocessing

fMRI preprocessing was performed using both AFNI (http://afni.nimh.nih.gov) and FSL (http://www.fmrib.ox.ac.uk/fsl/). Functional images were converted to 4D NIfTI format and corrected for slice-timing offsets. Motion correction was carried out using the AFNI program *3dvolreg*, with the reference volume set to the mean image of the first run in the series. Images were then smoothed with a 5 mm FWHM Gaussian kernel. Co-registration was performed with the AFNI program *3dAllineate* using the local Pearson correlation cost function optimized for fMRI-to-MRI structural alignment. The subsequent inverse transformation was then used to warp the anatomical image to the functional image space. Anatomical images were normalized using the FSL program *fnirt* to a standard volume (MNI_N27) available from the Montreal Neurological Institute (MNI; http://www.bic.mni.mcgill.ca). The same normalization parameters were later applied to native-space statistical maps as necessary for the generation of group statistical maps (see below).

Univariate analysis

To address a series of hypotheses, we carried out a number of voxel-wise fMRI statistical analyses for each subject using the general linear model (GLM) framework implemented in the AFNI program *3dDeconvolve*. The overall effects of motion coherence were assessed by modeling the six coherence values with separate regressors, each of which was derived by convolving a gamma probability density function (peaking at 6 s) with a vector of stimulus onsets for each condition. Tests of linear trends were carried out for each voxel using the coherence vector transformed to zero mean and a sum of squares equal to one (Kayser et al., 2010a), then applied to the estimated beta coefficients computed for each motion coherence value. The resulting values were subject to group level analyses, then mapped to the spatially normalized cortical surface.

Because we collected a large amount of data on a relatively small number of subjects, statistical power with respect to the parametric effect of motion coherence was relatively weak at the group level as compared with the single-subject level. Thus for the purposes of whole-brain images showing a group activation summary, we assessed significance using a fixed effects summary statistic with an overlap requirement (Friston et al., 1999). We computed a t-statistic for the linear contrast for every voxel in the volume and divided this value by the square root of the number of subjects (n = 7) (McNamee and Lazar, 2004), which was compared against a standard normal null distribution using an alpha value of $p = 0.0005$ for the full group. We also required that for a voxel to be declared significant, at least 4 out of 7 subjects show a significant effect ($p < 0.005$, uncorrected) at the single subject level. Unthresholded maps of the parametric effect of motion coherence then formed the inputs for whole-brain 1- and 2-way fixed-effects ANOVAs ($p < 0.0005$) using the same overlap requirement as above.

ROI selection

To avoid an ROI selection bias, fMRI data derived from a task training session performed in the MRI scanner were analyzed independently from the primary data set to generate regions of interest. ROIs were selected from those regions that showed negative parametric effects within either the stimulus or response phase, along with a positive main effect of task. Specifically, after single subject maps were normalized to MNI space, local maxima were defined on the fixed effects group map for the parametric effect (threshold at $p < 0.005$, uncorrected). Each defined maximum served as the center of a sphere with a diameter of 12 mm. In cases in which neighboring spheres showed any overlap, the sphere with the lesser maximum was excluded. After reverse-normalizing the ROIs to each subject's native space, we selected the top ten voxels from the training data set within each ROI that (1) demonstrated a positive main effect of task and (2) showed the maximal negative parametric variation for coherent motion. Each of these sets of voxels was then applied to the primary (and independent) data set.

BOLD time course estimation

Estimates of the hemodynamic responses from the onset of the stimulus phase through the response phase were calculated for each prior information state and motion coherence within an ROI. To produce an unbiased estimate of the time course, we applied a deconvolution approach to the main data set using piecewise b-spline basis functions (Saad et al., 2006) separated by 2 s intervals for 20 s after onset using AFNI's 3dDeconvolve command. Since trial onset times were not synchronous with the transistor–transistor logic (TTL) pulse, across the entire run we were able to sample the time course at a number of different points. To select and label the relevant time courses at each voxel, ROIs were reverse normalized to each subject's native space.

To distinguish between the timing of activity related to either Stimulus or Response phase, we selected the timing of the peak of occipital pole (OPOLE) activity to define the Stimulus phase, and the timing of the peak of primary motor cortex (M1) activity to define the Response phase. For these two ROIs, peak amplitude was defined as the largest mean percent BOLD change across coherence and task

type, and time to peak was defined as the time from trial onset to this maximum amplitude. Standard deviation across subject was calculated to account for variability in time-to-peak. The resulting values for these regions were 5.1 s ± 0.49 s for OPOLE and 9.9 s ± 1.34 s for M1. For subsequent ROIs, mean time courses across all subjects were examined for significant parametric effects at each time point across the duration of the trial. Maximal parametric effect was defined at the time of the most significant negative parametric effect for each time course, and peak amplitude was defined at the time of the largest mean percent BOLD change of the time course across coherence, irrespective of parametric effect.

Results

To temporally dissociate activity consistent with sensory processing and evidence accumulation from activity related to motor planning and response, we collected whole-brain fMRI data from seven highly trained subjects performing a delayed-response motion discrimination task. Subjects were first prompted with response-relevant information (2 s), after which they viewed a stimulus (2 s) consisting of upward or downward dot motion at a consistent coherence (but variable across trials) (Fig. 1). The prompt contained either information on modality and mapping (All), modality only (Modality) or no information (None). During the delayed response phase (2 s), the remaining information was given, while prior information was not repeated. Subjects were instructed to produce either a "left" or "right" response using the appropriate motor action as directed by the relevant prompt (either button press or saccade). Through this task design, stimulus- and response-related activity could be distinguished.

Behavioral performance

Subject behavioral performance was separated by prior information state and response modality (Fig. 2). For all modalities and prior information states, an increase in accuracy was observed as motion coherence increased ($F(4,24) = 63.81$, $p < <0.001$). An effect of prior information state on accuracy ($F(2,12) = 5.11$, $p = 0.025$) was driven by a significant difference at 2% coherence for button presses only. No significant differences in response times following the delay were observed across coherence ($F(4,24) = 0.58$, $p = 0.681$), though as expected, response times for both modalities became faster with increasing prior information ($F(2,12) = 25.84$, $p < <0.001$). Response times for saccades and button presses were different ($F(1,6) = 185.54$, $p < <0.0001$) due to the conservative threshold necessary for defining correct saccadic responses that likely overestimated eye response times (see Methods section). Importantly, no significant difference in accuracy was seen across modality ($F(1,6) = 0.0042$, $p = 0.95$). Since accuracies did not differ across modality and our hypotheses did not depend upon modality, we collapsed across hand and eye responses in subsequent analyses to increase statistical power.

Parametric effects of coherence

To identify areas in which activity varied with motion coherence, we examined linear contrasts testing for a parametric effect of coherence within each prior information state (All, Modality, None) for the two trial phases (Stimulus, Response). In the Stimulus phase, activity varied inversely with motion coherence within a network similar to our previous findings (Fig. 3A; all surfaces thresholded at $p < 0.0005$ uncorrected with an overlap requirement; see Methods section). Prominent parametric activations were seen in MT+, the intraparietal sulcus (IPS), frontal eye fields (FEF), supplementary motor area (SMA), middle frontal gyrus (MFG), and anterior insula (aINS), among other regions (Table 1), consistent with previous work (Hebart et al., 2012; Ho et al., 2009; Kayser et al., 2010a,b; Liu and Pleskac, 2011; Tosoni et al., 2008). To examine the influence of prior information state on the parametric effect during the Stimulus phase, we performed a whole-brain one-way ANOVA (Fig. 3B). The results showed that this negative parametric activity did not differ significantly across prior information states, indicating that this activity was independent of prior information state.

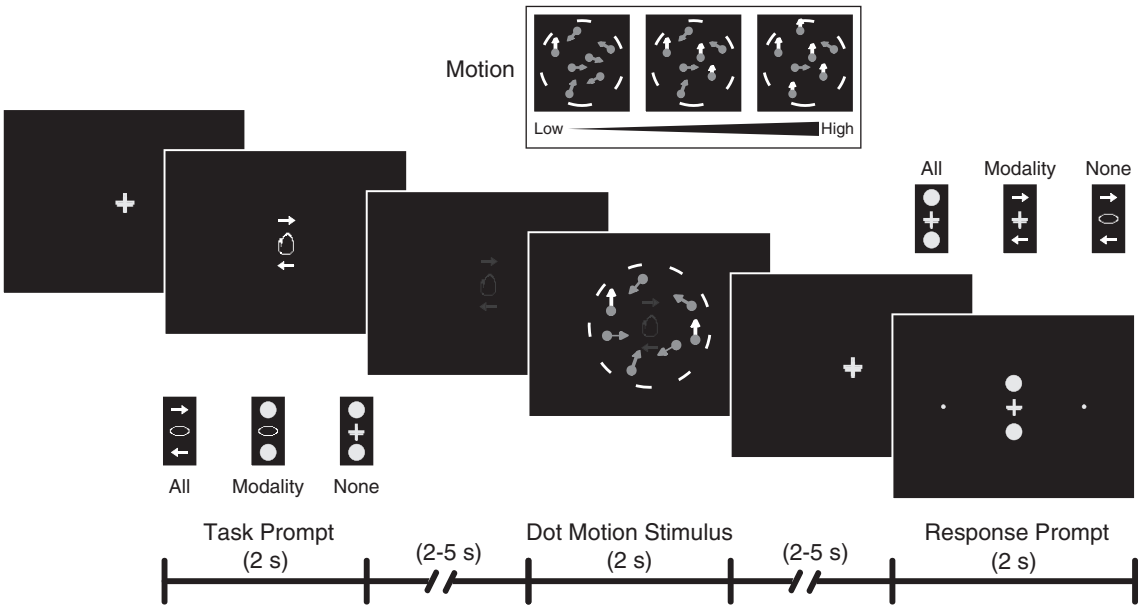

Fig. 1. Bi-modality dot motion discrimination task. Each run began with a prompt consisting of symbols that represented response modality and response mapping information (All), only response modality information (Modality), or neither (None). An eye symbol represented saccadic responses, while a hand symbol represented button press responses. Arrows pointing left or right were positioned above and below central fixation to indicate the mapping of upward/downward dot direction to a response (see Methods section). When no information for modality and/or mapping was provided, the symbols were replaced by a fixation cross and filled circles, respectively. The symbols were then dimmed for a jittered interval, followed by the presentation of a dot motion stimulus within a central circular aperture of 7.5° diameter (dashed circle) for 2 s. Each dot stimulus moved upward or downward with a motion coherence value of 0%, 2%, 4%, 16%, 32%, or 100%. After a jittered interval in which only a central fixation cross was present, a response prompt appeared with the remaining response information, as well as two circular targets displayed 10° to the left and right of central fixation. Subjects made their response during this interval with either a button press or saccade, as directed by the modality and mapping information.

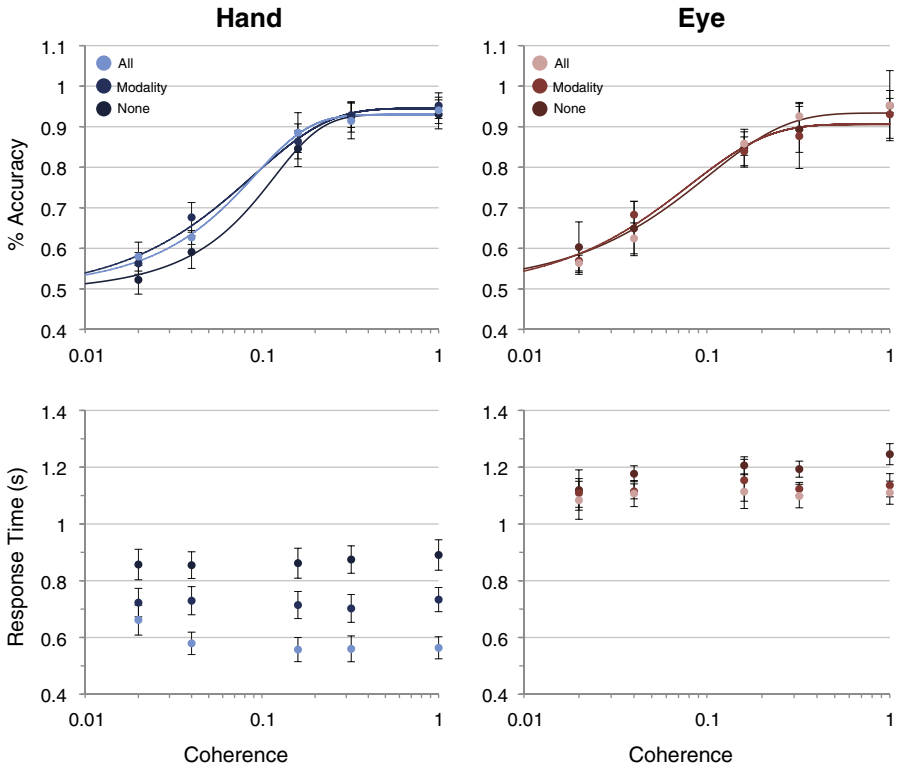

Fig. 2. Subject accuracies and response times for both response modalities (hand, eye) across motion coherence of 0%, 2%, 4%, 16%, 32%, and 100%. Response times for hand were recorded by button press, while response times for eye were recorded by eye tracker (see Methods section). Responses are separated by information state (All, Modality, None). Error bars denote standard error of the mean across the seven subjects.

During the Response phase, we also found areas that demonstrated an inverse parametric effect of motion coherence (Fig. 3A). These regions were fewer than in the Stimulus phase, but included IPS, MFG, and aINS. The motion-sensitive area (MT+) was not present, consistent with the absence of the stimulus during this phase. Notably, during trials with no prior information (None), no significant negative parametric activity was present during the Response phase, consistent with this negative parametric effect not being directly related to the stimulus. To confirm this influence of prior information state, we performed a one-way ANOVA across prior information state during the Response phase. The results showed significant differences in parametric activity within IPS, MFG, and aINS (Fig. 3B), consistent with the idea that this activity, unlike the Stimulus phase activity, was dependent on prior information.

To examine changes in parametric effect between the two phases, we conducted a one-way ANOVA across trial phase for each of the prior information states (Fig. 3C). While some differences were observed, differences in IPS, MFG and aINS were consistently present only for trials with no prior information (None). A whole-brain two-way ANOVA across trial phase and information state was performed to identify areas in which the differences in parametric effect showed an interaction between phase and prior information state (Fig. 3D). The most notable significant effect was found in IPS, implicating this region in linking stimulus activity with information about the response.

ROI time course analysis

To further investigate how BOLD activity varied across the task, we used an independent set of task data within each subject to identify regions of interest. We focused our examination on voxels from ROIs in which activity demonstrated a negative parametric effect within either Stimulus or Response phase in the independent data set (MT+ from Stimulus phase, SMA from Response phase) and that were important to the task based on previous findings (IPS from Stimulus phase, IPS from Response phase). These voxels were then applied to the primary data set for analysis. As references, activity was examined within two areas that did not vary parametrically with motion coherence and that represented early sensory and late motor processing: primary visual cortex (the occipital pole, or OPOLE) and a primary motor area (M1). Specifically, when evaluating time courses, we considered the range of peak activity within OPOLE and M1 to define the epoch from the Stimulus phase (5.1 s ± .49 s) to the Response phase (9.9 s ± 1.34 s), respectively (Fig. 4, black dotted lines).

To address our hypothesis that regions important for sensorimotor transformations should show a negative parametric effect of motion coherence when the stimulus is present, and a dissociable peak of activity that tracks the timing of motor planning, we evaluated the time course of BOLD activity for each motion coherence level from Stimulus onset through Response phase (Fig. 4). To determine when the parametric effect of motion coherence was most significant during the trial, we analyzed the parametric effect at each time point of the time course, and determined the timing of the maximum negative parametric effect (light blue dash–dotted line). These results were then compared to the Stimulus and Response activity references (Fig. 5A). Confirming the BOLD results, MT+ and Stimulus-selected IPS showed a significant negative parametric effect ($p < 0.05$) in the Stimulus phase for each prior information state that reached maximal significance in or closest to the range of peak Stimulus phase. Parametric activity in MT+ appeared to strongly differentiate the 100% motion coherence stimulus, while time courses in Stimulus-selected IPS showed a broader distribution of motion coherence responses. SMA and Response-selected IPS showed negative parametric effects that were maximal later for trials with prior information (All, Modality), but no significant parametric effect was observed for trials without prior information (None), strongly differentiating the ROIs as well as this information state (Fig. 4, lower right).

The peak amplitude of the time course was also examined along with the maximal parametric effect, and the consistency of their

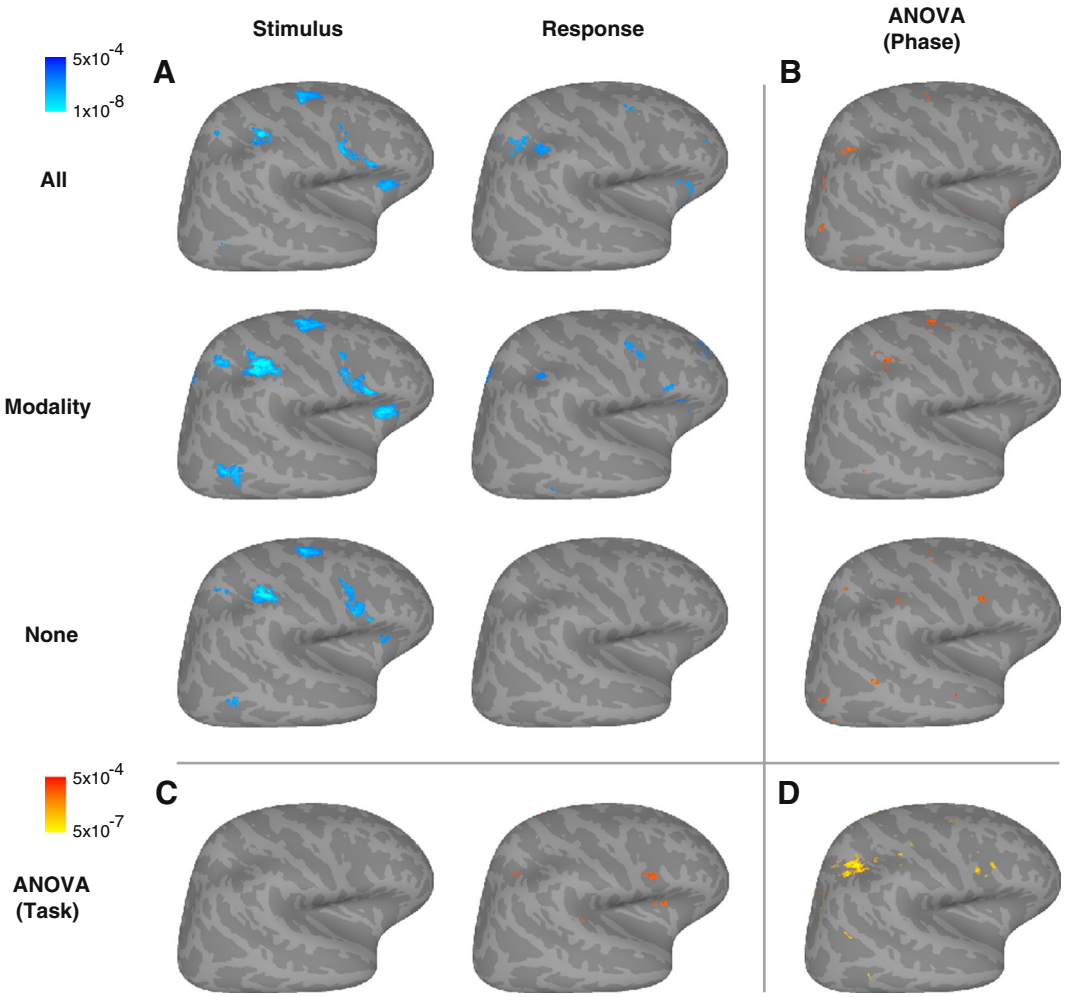

Fig. 3. A: Parametric effect of motion coherence for the Stimulus and Response phases of the task, separated by information state (All, Modality, None). Displayed activity represents negative parametric variation (blue color scale, $p < 0.0005$) that was significant in at least 4 of 7 subjects and was found within areas of positive main effect of task. B: One-way ANOVAs for each information state (All, Modality, None) across Stimulus and Response phases. Displayed values represent voxels with significant differences across phases (red-yellow color scale, $p < 0.0005$). C: One-way ANOVAs for each task phase (Stimulus, Response) across information states (All, Modality, and None; $p < 0.0005$). D: Two-way ANOVA illustrating the interaction between phase and information states ($p < 0.0005$). All assessments of significance for ANOVAs also included an overlap requirement of 4 of 7 subjects (see Methods section).

timing was compared (Fig. 4, dark blue dash–dotted lines). Activity within the sensory area MT+ peaked during the Stimulus phase for all prior information states, and activity within SMA peaked during the Response phase for all prior information states (Fig. 5B), similar to the maximal parametric effect. In contrast, time courses for Stimulus- and Response-selected IPS ROIs showed a shift in the peak amplitude across prior information states. Specifically, as prior information decreased, thus shifting motor planning into the Response phase, time courses for both Stimulus- and Response-selected IPS ROIs demonstrated a concurrent shift in the peak amplitude to the Response phase. However, in the Stimulus-selected IPS ROI, the parametric effect remained maximal in the Stimulus phase. Thus, the maximal parametric effect dissociated from the peak amplitude of the time course in this region, consistent with activity related to sensorimotor transformations.

Along with Stimulus-selected-IPS, we also examined other Stimulus-selected regions (Fig. 5, gray bars) that were determined to be part of the decision network in our previous work (Kayser et al., 2010a,b). As above, we evaluated the timing of both the maximal parametric effect and the peak time course amplitude. The time course in IFS, which was previously shown to influence IPS activity (Kayser et al., 2010b), showed a peak amplitude that remained strongest within the Stimulus phase for all prior information states, and did not dissociate from the parametric effect. Two other areas, aINS and pSMA, also showed a dissociation of maximum activity from parametric effect, though the peak amplitude did not shift to the Response phase until no prior information trials (None). These findings suggest that while Stimulus-selected-IPS is not the only area to show a temporal dissociation between maximum parametric effect and peak amplitude, its activity more closely tracks both sensory evidence during the Stimulus phase, and the shift of motor planning from the Stimulus to Response phase.

Discussion

By dissociating sensory processing from motor planning and response, we demonstrated that IPS couples these cognitive components in a manner consistent with sensorimotor transformations. While stimulus-related processing and activity relevant to motor planning and response occurred in many regions within the network, certain regions showed activity whose timing covaried with prior information state. In particular, a region in IPS previously identified as a potentially important area for evidence accumulation by the presence of a parametric effect of stimulus also displayed activity that peaked in association with motor planning. Thus, IPS appears to play an important role in both processes during perceptual decisions, and is a likely candidate to mediate the transformation from stimulus to response.

Table 1
Areas showing a significant parametric effect with respect to motion coherence for the listed phase and task, in MNI coordinates. Each section only includes areas whose main effect of task was positive (i.e., that activated during stimulus presentation). "Overlap" indicates the number of individual subjects who showed significant univariate effects within each region. No regions demonstrated a significant parametric effect in the Response phase of the None condition.

RRegion	Hemi	X	Y	Z	T-value	Overlap
Stimulus phase — All						
MT+	L	−55	−70	9	−7.07	7
pOCC	R	13	−103	10	−6.09	7
FEF	R	29	−7	52	−12.14	6
PoG	R	44	−30	45	−10.9	6
SMA	M	7	17	51	−8.83	6
MT+	R	51	−67	4	−8.3	6
sOCC	L	−15	−99	14	−6.72	6
IFS	R	57	12	30	−9.92	5
IFS	R	52	9	15	−8.54	5
aINS	R	32	26	2	−7.74	5
SMA	M	−10	17	42	−6.7	5
aIPS	L	−28	−57	63	−6.48	5
mIPS	R	20	−60	48	−6.07	5
SMA	R	15	−2	67	−5.85	5
aINS	L	−34	18	4	−5.77	5
aIPS	R	43	−47	60	−7.42	4
FEF	L	−34	−4	56	−6.19	4
PoG	R	60	−12	27	−5.97	4
Stimulus phase — Modality						
MT+	R	51	−68	2	−10.32	7
aIPS	L	−28	−56	59	−8.35	7
PoG	R	42	−29	42	−14.24	6
FEF	R	28	−6	52	−11.87	6
IFS	R	54	11	15	−10.36	6
SMA	M	7	7	55	−9.81	6
aINS	R	32	24	5	−9.54	6
FEF	L	−26	−4	53	−8.41	6
IFS	L	−45	0	37	−8.03	6
dOCC	L	−25	−74	20	−5.78	6
pOCC	R	30	−84	41	−5.49	6
SMA	M	−5	16	48	−11.19	5
aIPS	R	36	−52	58	−9.89	5
aINS	L	−31	17	7	−8.95	5
IFS	L	−55	9	16	−7.75	5
mIPS	R	19	−69	54	−6.97	5
IFS	R	43	1	34	−6.64	5
SMA	L	−9	−1	57	−6.5	5
IFS	R	58	9	33	−9.66	4
MT+	L	−49	−68	4	−8.42	4
ACC	M	8	23	33	−7.87	4
FEF	L	−48	−3	54	−7.57	4
IPL	L	−35	−39	41	−7.18	4
PoG	R	62	−19	39	−6.49	4
sOCC	L	−5	−102	8	−6.4	4
ACC	L	−9	29	29	−6.19	4
IPL	L	−48	−29	37	−5.95	4
FEF	R	29	3	68	−5.77	4
sOCC	L	−14	−96	22	−5.54	4
Stimulus phase — None						
MT+	R	49	−66	1	−9.71	7
IFS	L	−42	−1	50	−6.95	7
PoG	R	45	−28	41	−13.03	6
FEF	R	25	−8	48	−10.53	6
SMA	R	8	17	49	−8.38	6
MT+	L	−50	−68	4	−7.78	6
IFS	L	−52	4	38	−6.73	6
IPL	L	−36	−40	43	−5.6	6
mIPS	R	20	−67	55	−5.41	6
IFS	R	53	8	32	−8.58	5
aIPS	L	−35	−53	61	−7.48	5
aIPS	R	40	−42	52	−7.47	5
aINS	R	34	26	4	−6.4	5
SMA	M	3	9	63	−6.29	5
aINS	L	−31	17	11	−5.86	5
SMA	L	−9	15	43	−5.69	5
IFS	R	52	8	15	−8.76	4
PoG	R	59	−21	35	−6.85	4
FEF	L	−28	−4	60	−6.63	4
IFS	R	36	2	35	−6.3	4
IFS	L	−56	6	17	−6.09	4
Response phase – All						
SMA	M	1	18	48	−8.95	7
aINS	L	−32	25	6	−7.82	7
ACC	M	−8	28	26	−7.09	7
pOCC	R	17	−74	36	−7.02	7
aIPS	L	−31	−60	56	−6.85	7
mIPS	L	−15	−72	55	−6.72	7
IPL	L	−43	−35	39	−6.53	7
IPL	R	42	−37	46	−6.52	7
aOCC	R	23	−59	18	−6.32	7
IFG	R	35	27	−6	−6.03	7
pOCC	L	−17	−79	38	−5.66	7
IFS	R	43	7	46	−5.56	7
aIPS	L	−37	−46	50	−5.45	7
OFC	R	25	44	−16	−5.45	7
dOCC	R	36	−74	37	−5.31	7
pCun	R	9	−51	53	−5.22	7
FPC	L	−30	58	16	−7.32	6
FEF	R	32	2	65	−7.23	6
IFS	L	−44	2	35	−6.97	6
FEF	L	−30	1	55	−6.9	6
aIPS	R	26	−46	48	−6.43	6
IFG	L	−45	19	−7	−6.23	6
PoG	R	50	−36	60	−5.68	6
ACC	M	6	34	31	−5.39	6
mIPS	R	14	−75	53	−5.33	6
IFG	L	−44	22	28	−5.55	5
Thal	L	−8	−17	12	−5.88	4
Response phase — Modality						
MFG	R	38	43	22	−5.95	7
SMA	M	0	18	59	−7.48	6
ACC	M	−2	23	35	−6.95	6
ACC	M	−4	37	24	−5.89	6
IFG	R	52	14	21	−5.86	6
IFG	L	−31	30	4	−5.79	6
IFS	L	−48	5	33	−5.71	6
aINS	L	−32	15	14	−5.65	6
mIPS	L	−20	−63	46	−5.65	6
mIPS	R	21	−65	56	−5.61	6
aINS	L	−43	16	−1	−5.53	6
IFS	R	44	3	41	−5.51	6
MFG	R	44	8	59	−5.45	6
IPL	R	41	−38	37	−5.23	6
SFG	L	−22	46	24	−6.62	5
FPC	R	29	60	−7	−6.25	5
IPL	L	−64	−43	34	−5.8	5
MFG	L	−37	35	32	−5.43	5
FPC	L	−31	58	12	−5.42	5
FPC	R	23	60	24	−5.37	5
MT+	R	56	−54	−11	−5.36	5
SMA	L	−15	6	62	−5.22	5

Previous work in primates has also suggested that IPS is important for sensorimotor transformations, rather than exclusively sensory or motor representations. Neuronal activity within the macaque homologue of mIPS, the lateral intraparietal area (LIP; Grefkes and Fink, 2005), correlated with the predictions of a diffusion model for evidence accumulation to threshold (Roitman and Shadlen, 2002; Shadlen and Newsome, 2001), thereby linking sensory information with the response. Moreover, microstimulation of LIP neurons that showed accumulation-related activity toward a specific direction increased the choice of that direction only when the stimulus was presented (Hanks et al., 2006), indicating that this area requires sensory information to influence motor response. To further define the relationship between evidence accumulation and motor planning in LIP, a recent study used a dot motion direction task with response information provided before, during, or after the motion stimulus (Bennur and Gold, 2011). Motion direction-selective LIP neurons showed parametric activity that correlated with motion coherence and peak neural activity that correlated with motor planning. Significantly,

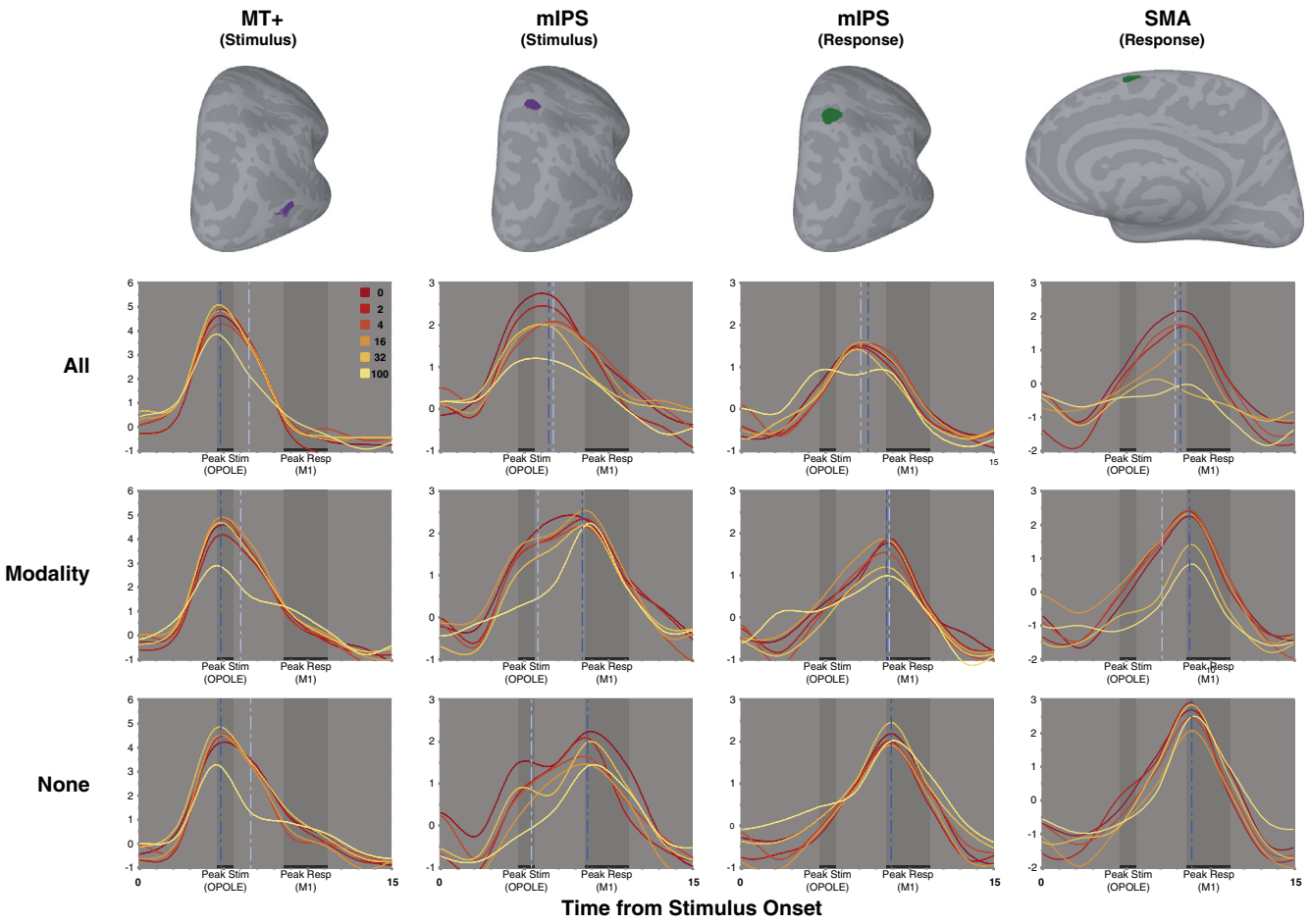

Fig. 4. Time courses of independently selected ROIs, separated by motion coherence and information state. Colored areas on the surfaces represent ROIs defined within either Stimulus (purple) or Response (green) phase. Red-yellow colored curves represent time courses from the onset of stimulus phase through response phase, for 0%, 2%, 4%, 16%, 32% and 100% motion coherence. Time from onset for peak Stimulus and peak Response phase activity (darkened regions) was determined based on peak activity of OPOLE (at 5.1 s ± 0.492 s) and M1 (at 9.9 s ± 1.34 s), respectively (see Methods section). Maximum parametric activity (light blue dash–dotted line) was calculated from analysis of parametric effect across coherence at each time point of the curves. Peak amplitude (dark blue dash–dotted line) was calculated from peak BOLD activity averaged across coherence. Note that for Response-defined mIPS and SMA in the None condition, there were no times during which the parametric effect was significant, and thus no maximum parametric activity.

these activities were shown to be dissociable when the task varied the timing of the motor planning information. Consistent with our present findings, these results in macaques demonstrate that LIP activity is related to both sensory and motor components of a decision.

From studies that examine the human IPS, it is apparent that the human region is also well positioned to play a key role in sensorimotor transformations. Functional connectivity analyses have shown a tight correlation between visual cortex and IPS activity during visuospatial processing (Kayser et al., 2010a; Sereno et al., 2001; Silver et al., 2005; Swisher et al., 2007), and manipulation of visuospatial or feature-based attention modulates IPS activity (Corbetta and Shulman, 2002; Kayser et al., 2010b, respectively). Further studies have also correlated IPS activity with evidence accumulation (Kayser et al., 2010a; Ploran et al., 2007) and motor intention (Hesse et al., 2006; Rushworth et al., 2003); and a number of studies investigating visuomotor control show activation within and around IPS (reviewed in Culham et al., 2006).

More recently, reports using independent methods such as diffusion tensor imaging and resting state analyses to define parietal subregions have identified areas homologous to the right mIPS region characterized in our stimulus phase (mean MNI coordinates [20–65 52]). Mars et al. (2011), for example, defined a region located at [19–67 53] that overlaps with human area 7A and lies close to the IPS3 retinotopic map. In addition to demonstrating that this regions shares resting state connectivity with MT+ and presumptive FEF, they noted that its activity is thought to reflect visual attentional signals and shares similarities with signals in macaque area LIP. Likewise, Nelson et al. (2010) identified a right medial IPS region at [18–64 59] that was part of an IPS/dlPFC submodule implicated in attentional control. Finally, in a study of motion and eye movement selectivity, Konen and Kastner (2008) found a nearby region (MNI coordinates [28–67 53]) that also encompassed IPS3, was strongly motion selective, and included spatial attention signals.

Consistent with these findings, a region identified in the more anterior IPS in the current study (mean MNI coordinates [36–47 55]) could also be found near areas identified in the Mars ([30–41 53]) and Nelson ([32–51 48]) reports (although it was more anterior than the regions studied by Konen and Kastner). As for the medial IPS region above, these regions demonstrated resting state functional connectivity with MT+ and FEF (Mars et al., 2011) and were part of the IPS/dlPFC submodule (Nelson et al., 2010), respectively. In keeping with the similarities in the parcellation of these middle and anterior IPS areas, the anterior IPS region was implicated in motion processing and attentional control. Taken together, these studies identifying strong visual attention and motion selectivity signals in overlapping or closely adjacent parietal areas support our finding that IPS may be integral to the transformation between sensory and motor representations.

Importantly, our task design distinguishes sensorimotor transformations from other possible explanations that do not easily explain our results, such as task difficulty related to the coherence manipulation. Of course, task difficulty does not represent a cognitive process in and of itself; rather, it serves as a proxy for other cognitive processes

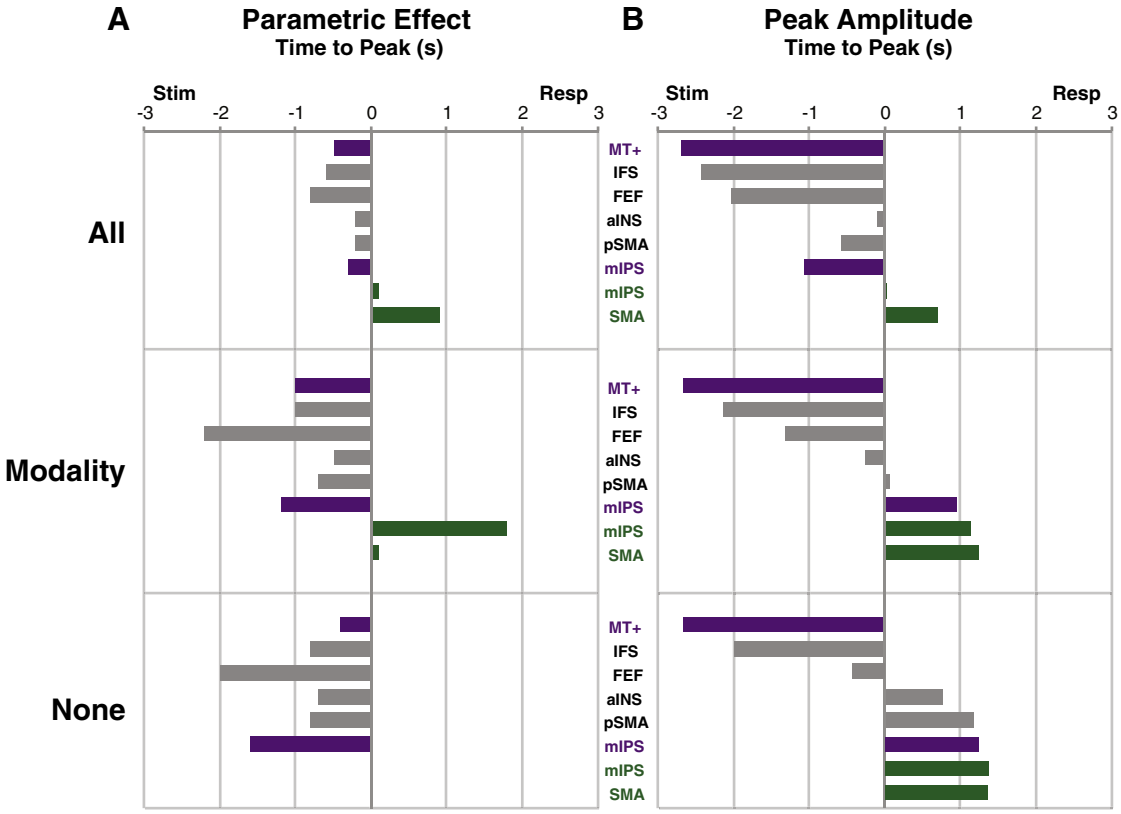

Fig. 5. Activity summary across ROIs, including Stimulus-selected MT+ (purple), Stimulus-selected mIPS (purple), Response-selected mIPS (green), and Response-selected SMA (green). A: Timing of maximum parametric effect in the time course. To illustrate the timing of this maximum with respect to the Stimulus and Response phase, the time point of the maximum parametric effect was subtracted from the time point halfway between peak Stimulus phase and peak Response phase (7.5 s; see Methods section), segregated by information state (All, Modality, None). B: Timing of peak amplitude in the time course. The time point of the peak amplitude was subtracted from the time point halfway between peak Stimulus phase and peak Response phase, segregated by information state (All, Modality, None).

such as perceptual salience or response uncertainty (Grinband et al., 2006; Kayser et al., 2010a). With respect to these processes, perceptual salience, for example, might give rise to a parametric BOLD effect during the Stimulus phase; but it would not easily explain nonparametric peak activity during the response phase, when the stimulus is absent. Likewise, attention to the stimulus might be parametric during the stimulus phase (though anticipatory attention related to the response signal would not), and attention to motor plans might be non-parametric during the response phase; but it is not clear that attention to sensory inputs and motor outputs would be equivalent processes found in the same (in this case, a parietal rather than a lateral frontal) brain region. In contrast, response uncertainty might demonstrate a parametric effect during the Response phase, depending upon the available evidence, but it would be less likely to do so during the Stimulus phase when the modality and mapping of the response are unknown. Unlike the specific predictions generated for the sensorimotor transformation hypothesis, none of these difficulty-related processes easily explains why activity should show both a parametric effect of stimulus and a non-parametric effect of response within the same region. More importantly, large changes in activity are seen in the Response phase across prior information state, independent of the coherence manipulation. Thus, the explanation that this activity represents sensorimotor transformations might be a more parsimonious hypothesis, supported by the aforementioned behavioral, neural, and computational data in primates and humans.

Several recent innovative studies have examined distinct but related questions about the role of IPS, including investigations into evidence accumulation. To better determine the influence of response modality in IPS and other regions, Ho and colleagues used the predictions of a linear ballistic accumulator model to hypothesize that an initial decrease in BOLD activity for low motion coherence trials compared to high motion coherence trials would identify evidence accumulator regions (Ho et al., 2009). They examined the time course of activity in regions such as IPS, aINS, and FEF for this initial relative decrease. For IPS, they only saw this effect during saccadic responses, and due to the lack of a consistent effect across modality, they attributed this finding to a more prominent role of IPS in motor planning. Although we found a consistent response from IPS across modalities, we also identified an initial decrease in BOLD activity for lower motion coherences, most prominently in trials with some or no prior response information (Modality, None; Fig. 4). It is possible that this accumulation-associated effect was not seen in the All condition of the current study because it was partially masked by concurrent activity associated with motor planning. Thus, dissociation of stimulus and response may be important to unraveling the role that IPS plays in the transformation from one to the other.

Other studies have attempted to dissociate sensory from motor activity. Recent elegant work by Tosoni and colleagues examined IPS activity using a visual discrimination task with two response modalities and a delayed response (Tosoni et al., 2008). Their results showed that activity within IPS at the stimulus presentation correlated with evidence accumulation, while no correlation was identified during the response period. However, because subjects were informed of the upcoming response mapping prior to stimulus presentation, it is possible that motor planning could be completed during the stimulus phase. In a similar study, Liu and Pleskac used a dot motion task with two levels of motion coherence that required button presses or saccades, but included trials in which the modality for response was provided after the stimulus phase (Liu and Pleskac, 2011). Their important results

showed that the effect of two levels of motion coherence on IPS activity was independent of modality, but they did not report any differences in activity across prior information states. It is possible that such differences could be more difficult to detect without the sensitivity provided by a parametrically varied motion stimulus. Additionally, the perfect correspondence between direction of the stimulus and the response could potentially allow for planning of congruent responses in both modalities prior to knowledge of modality, thereby reducing motor planning differences between trials with and without prior modality knowledge. By decoupling motion direction from the response direction in the current experiment, we eliminated this possibility by introducing another level of prior information: response mapping. Specifically, since the Modality only condition does not define how the motion stimulus maps to opposing left/right responses, we hypothesized that, compared to the All condition, motor planning would be delayed until the response prompt. As our results illustrate, withholding response mapping alone, even when response modality was known, led to a shift in peak activity within IPS towards the Response phase, while the effect of motion coherence, consistent with the above findings, remained within the Stimulus phase.

Of course, other regions beyond IPS are also likely to be involved in sensorimotor transformations. A recent examination of activity across the macaque cortex during a delayed vibrotactile comparison task demonstrated that activity during the first sensory input was found beyond primary somatosensory cortex (S1) in ventral premotor (VPC), medial premotor (MPC), and prefrontal cortex (PFC) (Hernandez et al., 2010). Only those regions outside S1 showed activity correlated with sensory comparisons and motor planning during presentation of the second sensory input. Thus, by dissociating early sensory processing and motor planning, this task illustrated that sensory-related activity was present in a number of regions that also displayed activity related to motor planning and response. In keeping with this finding, we identified two additional Stimulus-selected regions, aINS and pSMA, that showed dissociable Stimulus and Response phase activity (Fig. 5). These regions closely overlap regions within the core network responsible for task set maintenance identified by Dosenbach et al. (2006), and one possibility is that they monitor sensorimotor transformations occurring within IPS. pSMA, which is additionally involved with learning and planning complex motor actions (reviewed in Nachev et al., 2008), might also participate in planning the resulting motor response.

In addition to the parametric effects observed in the above regions during the Stimulus phase, other regions were shown to have a parametric activity during the Response phase when some prior information was known. If the parametric effect is not required for motor planning, then why does it persist into the Response phase when some prior response information is present? It is possible that this effect represents sensory information retained into the Response phase. However, the fact that this parametric effect is not seen in the Response phase when no prior information is provided argues that, at a minimum, this activity is not solely tied to stimulus representations. Another possibility is that it reflects uncertainty in the motor response, which would be uniform, and therefore non-parametric, when no prior information is provided. However, motor planning also distinguishes the other two information states, yet no difference in parametric effect is observed. Therefore, this activity is also less likely to be solely tied to response representations. While this finding suggests a focus for further experiments, it also reinforces the idea that a parametric effect of coherence is necessary but not sufficient for a region to be involved in a process such as evidence accumulation. Moreover, it demonstrates that parametric responses are useful signals for defining regions involved in the decision making network.

In summary, these results demonstrate that neural activity consistent with stimulus-related and response-related components of a sensorimotor transformation can be temporally distinguished within a perceptual decision. Building upon previous studies, these findings directly implicate IPS in linking stimulus- and response-related processes within the brain, and argue that this region plays a key role in sensorimotor transformations.

Acknowledgments

This research was supported by startup funding from the State of California (A.S.K.). We thank Mark D'Esposito for scanner access, Kevin Japardi for help with data acquisition, Ana Navarro-Cebrian for helpful comments, and the subjects for their participation.

Conflict of interest statement

The authors report no conflicts of interest.

References

Amano, K., Wandell, B.A., Dumoulin, S.O., 2009. Visual field maps, population receptive field sizes, and visual field coverage in the human MT+ complex. J. Neurophysiol. 102, 2704–2718.
Andersen, R.A., Snyder, L.H., Bradley, D.C., Xing, J., 1997. Multimodal representation of space in the posterior parietal cortex and its use in planning movements. Annu. Rev. Neurosci. 20, 303–330.
Bennur, S., Gold, J.I., 2011. Distinct representations of a perceptual decision and the associated oculomotor plan in the monkey lateral intraparietal area. J. Neurosci. 31, 913–921.
Brainard, D.H., 1997. The psychophysics toolbox. Spat. Vis. 10, 433–436.
Corbetta, M., Shulman, G.L., 2002. Control of goal-directed and stimulus-driven attention in the brain. Nat. Rev. Neurosci. 3, 201–215.
Culham, J.C., Cavina-Pratesi, C., Singhal, A., 2006. The role of parietal cortex in visuomotor control: what have we learned from neuroimaging? Neuropsychologia 44, 2668–2684.
Dosenbach, N.U., Visscher, K.M., Palmer, E.D., Miezin, F.M., Wenger, K.K., Kang, H.C., Burgund, E.D., Grimes, A.L., Schlaggar, B.L., Petersen, S.E., 2006. A core system for the implementation of task sets. Neuron 50, 799–812.
Friston, K.J., Holmes, A.P., Price, C.J., Buchel, C., Worsley, K.J., 1999. Multisubject fMRI studies and conjunction analyses. NeuroImage 10, 385–396.
Gold, J.I., Shadlen, M.N., 2007. The neural basis of decision making. Annu. Rev. Neurosci. 30, 535–574.
Grefkes, C., Fink, G.R., 2005. The functional organization of the intraparietal sulcus in humans and monkeys. J. Anat. 207, 3–17.
Grinband, J., Hirsch, J., Ferrera, V.P., 2006. A neural representation of categorization uncertainty in the human brain. Neuron 49, 757–763.
Hanks, T.D., Ditterich, J., Shadlen, M.N., 2006. Microstimulation of macaque area LIP affects decision-making in a motion discrimination task. Nat. Neurosci. 9, 682–689.
Hebart, M.N., Donner, T.H., Haynes, J.D., 2012. Human visual and parietal cortex encode visual choices independent of motor plans. NeuroImage 63, 1393–1403.
Heekeren, H.R., Marrett, S., Ungerleider, L.G., 2008. The neural systems that mediate human perceptual decision making. Nat. Rev. Neurosci. 9, 467–479.
Hernandez, A., Nacher, V., Luna, R., Zainos, A., Lemus, L., Alvarez, M., Vazquez, Y., Camarillo, L., Romo, R., 2010. Decoding a perceptual decision process across cortex. Neuron 66, 300–314.
Hesse, M.D., Thiel, C.M., Stephan, K.E., Fink, G.R., 2006. The left parietal cortex and motor intention: an event-related functional magnetic resonance imaging study. Neuroscience 140, 1209–1221.
Ho, T.C., Brown, S., Serences, J.T., 2009. Domain general mechanisms of perceptual decision making in human cortex. J. Neurosci. 29, 8675–8687.
Kayser, A.S., Buchsbaum, B.R., Erickson, D.T., D'Esposito, M., 2010a. The functional anatomy of a perceptual decision in the human brain. J. Neurophysiol. 103, 1179–1194.
Kayser, A.S., Erickson, D.T., Buchsbaum, B.R., D'Esposito, M., 2010b. Neural representations of relevant and irrelevant features in perceptual decision making. J. Neurosci. 30, 15778–15789.
Konen, C.S., Kastner, S., 2008. Representation of eye movements and stimulus motion in topographically organized areas of human posterior parietal cortex. J. Neurosci. 28, 8361–8375.
Lee, J., Williford, T., Maunsell, J.H., 2007. Spatial attention and the latency of neuronal responses in macaque area V4. J. Neurosci. 27, 9632–9637.
Liu, T., Pleskac, T.J., 2011. Neural correlates of evidence accumulation in a perceptual decision task. J. Neurophysiol. 106, 2383–2398.
Mars, R.B., Jbabdi, S., O'Reilly, J.X., Croxson, P.L., Olivier, E., Noonan, M.P., Bergmann, C., Mitchell, A.S., Baxter, M.G., Behrens, T.E.J., Johansen-Berg, H., Tomassini, V., Miller, K.L., Rushworth, M.F.S., 2011. Diffusion-weighted imaging tractography-based parcellation of the human parietal cortex and comparison with human and macaque resting-state functional connectivity. J. Neurosci. 31, 4087–4100.
McNamee, R.L., Lazar, N.A., 2004. Assessing the sensitivity of fMRI group maps. NeuroImage 22, 920–931.
Mita, A., Mushiake, H., Shima, K., Matsuzaka, Y., Tanji, J., 2009. Interval time coding by neurons in the presupplementary and supplementary motor areas. Nat. Neurosci. 12, 502–507.
Nachev, P., Kennard, C., Husain, M., 2008. Functional role of the supplementary and pre-supplementary motor areas. Nat. Rev. Neurosci. 9, 856–869.
Nelson, S.M., Cohen, A.L., Power, J.D., Wig, G.S., Miezin, F.M., Wheeler, M.E., Velanova, K., Donaldson, D.I., Philips, J.S., Schlaggar, B.L., Petersen, S.E., 2010. A parcellation scheme for human left lateral parietal cortex. Neuron 67, 156–170.
Palmer, J., Huk, A.C., Shadlen, M.N., 2005. The effect of stimulus strength on the speed and accuracy of a perceptual decision. J. Vis. 5, 376–404.
Pelli, D.G., 1997. The VideoToolbox software for visual psychophysics: transforming numbers into movies. Spat. Vis. 10, 437–442.

Ploran, E.J., Nelson, S.M., Velanova, K., Donaldson, D.I., Petersen, S.E., Wheeler, M.E., 2007. Evidence accumulation and the moment of recognition: dissociating perceptual recognition processes using fMRI. J. Neurosci. 27 (44), 11912–11924.

Ploran, E.J., Tremmell, J.J., Nelson, S.M., Wheeler, M.E., 2011. High quality but limited quantity perceptual evidence produces neural accumulation in frontal and parietal cortex. Cereb. Cortex 21, 2650–2662.

Ratcliff, R., McKoon, G., 2008. The diffusion decision model: theory and data for two-choice decision tasks. Neural Comput. 20, 873–922.

Roitman, J.D., Shadlen, M.N., 2002. Response of neurons in the lateral intraparietal area during a combined visual discrimination reaction time task. J. Neurosci. 22, 9475–9489.

Rowe, J.B., Hughes, L.E., Nimmo-Smith, I., 2010. Action selection: a race model for selected and non-selected actions distinguishes the contribution of premotor and prefrontal areas to the selection of action. NeuroImage 51, 888–896.

Rushworth, M.F., Johansen-Berg, H., Göbel, S.M., Devlin, J.T., 2003. The left parietal and premotor cortices: motor attention and selection. Neuroimage 20, S89–100.

Saad, Z.S., Chen, G., Reynolds, R.C., Christidis, P.P., Hammett, K.R., Bellgowan, P.S., Cox, R.W., 2006. Functional imaging analysis contest (FIAC) analysis according to AFNI and SUMA. Hum. Brain Mapp. 27, 417–424.

Sereno, M.I., Pitzalis, S., Martinez, A., 2001. Mapping of contralateral space in retinotopic coordinates by a parietal cortical area in humans. Science 294, 1350–1354.

Shadlen, M.N., Newsome, W.T., 2001. Neural basis of a perceptual decision in the parietal cortex (area LIP) of the rhesus monkey. J. Neurophysiol. 86, 1916–1936.

Silver, M.A., Ress, D., Heeger, D.J., 2005. Topographic maps of visual spatial attention in human parietal cortex. J. Neurophysiol. 94, 1358–1371.

Silver, M.A., Shenav, A., D'Esposito, M., 2008. Cholinergic enhancement reduces spatial spread of visual responses in human early visual cortex. Neuron 60, 904–914.

Swisher, J.D., Halko, M.A., Merabet, L.B., McMains, S.A., Somers, D.C., 2007. Visual topography of human intraparietal sulcus. J. Neurosci. 27, 5326–5337.

Tosoni, A., Galati, G., Romani, G.L., Corbetta, M., 2008. Sensory-motor mechanisms in human parietal cortex underlie arbitrary visual decisions. Nat. Neurosci. 11, 1446–1453.